

## UC Irvine

### UC Irvine Previously Published Works

**Title**

Specific Heat of CeRhIn<sub>5</sub>: Pressure-Driven Transition from Antiferromagnetism to Heavy-Fermion Superconductivity

**Permalink**

<https://escholarship.org/uc/item/1n92h03x>

**Journal**

Journal of Superconductivity and Novel Magnetism, 15(5)

**ISSN**

1557-1939

**Authors**

Fisher, RA  
Bouquet, F  
Phillips, NE  
[et al.](#)

**Publication Date**

2002-10-01

**DOI**

10.1023/a:1021051004086

**Copyright Information**

This work is made available under the terms of a Creative Commons Attribution License, available at <https://creativecommons.org/licenses/by/4.0/>

Peer reviewed

# Specific Heat of CeRhIn<sub>5</sub>: Pressure-Driven Transition From Antiferromagnetism to Heavy-Fermion Superconductivity

R. A. Fisher,<sup>1,2</sup> F. Bouquet,<sup>1,2</sup> N. E. Phillips,<sup>1,2</sup> M. F. Hundley,<sup>3</sup>  
P. G. Pagliuso,<sup>3</sup> J. L. Sarrao,<sup>3</sup> Z. Fisk,<sup>4</sup> and J. D. Thompson<sup>3</sup>

---

CeRhIn<sub>5</sub> is known to show an unusual transition at a critical pressure of ~15 kbar. Specific-heat data show a gradual change in the zero-field “magnetic” specific-heat anomaly from one typical of antiferromagnetic ordering at ambient pressure to one more characteristic of a Kondo singlet ground state at 21 kbar. However, at 15 kbar there is a discontinuous change from an antiferromagnetic ground state to a superconducting ground state, and evidence of a weak thermodynamic first-order transition. Above the critical pressure, the low-energy excitations are characteristic of superconductivity with line nodes in the energy gap, and, at intermediate pressures, of extended gaplessness.

---

**KEY WORDS:** specific heat; pressure-driven transition; antiferromagnetism; superconductivity; heavy fermion.

---

The occurrence of superconducting (SC) heavy-fermion (HF) compounds provides a unique opportunity for investigating the relation between magnetism and superconductivity, particularly the possibility of magnetically mediated pairing of the electrons. In magnetic HF compounds there is a competition between magnetic order, driven by the RKKY interaction, and the spin-singlet ground state, favored by the Kondo interaction [1]. Both interactions are governed by the local-moment–conduction-electron exchange  $|J|$ , but the dependence on  $|J|$  is different, quadratic for the RKKY and exponential for the Kondo interaction. Since  $\partial|J|/\partial P > 0$ , the application of pressure ( $P$ ) can reduce the magnitude of the ordered magnetic moments and lower the ordering temperature. For appropriate values of the relevant parameters the Néel temperature ( $T_N$ ) of an antiferromagnetic (AF) HF

compound, and the Curie temperature ( $T_C$ ) of a ferromagnetic (FM) HF compound can be driven to zero at a critical pressure ( $P_c$ ). There has been considerable speculation that superconductivity might appear at that quantum critical point (QCP) with the electron pairing mediated by strong magnetic fluctuations, but the number of likely examples is small, presumably because the conditions that must be satisfied for superconductivity to be realized are so restrictive. Those conditions and the relevant concepts have been summarized in the context of the observed superconductivity in AF CePd<sub>2</sub>Si<sub>2</sub> and CeIn<sub>3</sub>, and a general phase diagram proposed [2]. The properties at AF and FM QCPs might be expected to be different, but, although the phase diagram for FM UGe<sub>2</sub> differs in detail from those for CePd<sub>2</sub>Si<sub>2</sub> and CeIn<sub>3</sub> [3], it is remarkably similar in general form. For all three of these materials the critical temperature for magnetic ordering approaches zero at  $P_c$ , and superconductivity appears in a narrow window of  $P$  with a strongly  $P$ -dependent critical temperature ( $T_c$ ), in accord with a model [2] in which a “continuous” transition at  $P_c$  is a condition for the occurrence of superconductivity. AF CeRhIn<sub>5</sub>, for which resistivity measurements have shown a phase diagram of a very different form [4], presents a striking

---

<sup>1</sup>Lawrence Berkeley National Laboratory, University of California, Berkeley, California 94720.

<sup>2</sup>Department of Chemistry, University of California, Berkeley, California 94720.

<sup>3</sup>Los Alamos National Laboratory, Los Alamos, New Mexico 87545.

<sup>4</sup>NHMFL, Florida State University, Tallahassee, Florida 32306.

contrast with those materials and with theoretical considerations generally:  $T_N \sim 4$  K, is only weakly dependent on  $P$  to 14.5 kbar, at the next higher  $P$ , 16.3 kbar, the signature of AF order has disappeared and superconductivity, with an essentially  $P$ -independent  $T_c$  of  $\sim 2$  K, appears. This phase diagram is qualitatively different from that of any other Ce HF compound, and, although the thermodynamic nature of the transition cannot be unequivocally determined from transport properties, the abrupt change at  $P_c$  suggests a “first-order-like transition” [4].

Measurements of the specific heat ( $C$ ) reported here show that the superconductivity is a bulk property, and characterize its nature. They determine the quasiparticle density of states and the nature of the other low-energy excitations, thereby identifying the ground states throughout the range of  $P$ . The ground states, AF below  $P_c$  and HF/SC above, both evolve continuously with increasing  $P$ , but at  $P_c$  there is a discontinuous change: Long-range AF order disappears and superconductivity appears.

Zero-field measurements of  $C$  are shown in Fig. 1 for representative values of  $P$ . (In all figures, results associated with the AF phase are represented by solid symbols, with the SC phase by open symbols.) The lattice heat capacity ( $C_{\text{lat}}$ ), taken to be the same as that of  $\text{LaRhIn}_5$  [4], and shown in Fig. 1, was subtracted from  $C$  to obtain the “electron” contribution ( $C_e$ ). With increasing  $P$  the “magnetic” specific-heat anomaly, which is associated with AF ordering at ambient pressure, becomes broadened and reduced

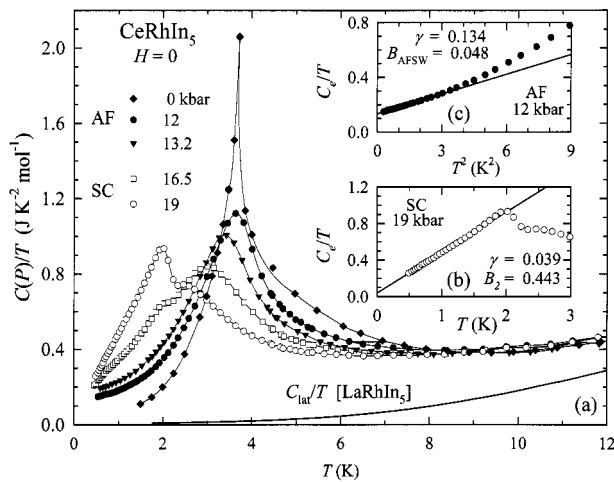


**Fig. 1.** (a) The specific heat, for representative values of  $P$ , as  $C/T$  vs.  $T$ . The  $P = 0$  data are from Ref. 4. The insets show  $C_e$  in the low- $T$  limit; (b) for  $P > P_c$ ,  $C_e = \gamma T + B_2 T^2$ ; (c) for  $P < P_c$ ,  $C_e = \gamma T + B_{\text{AFSW}} T^3$ .

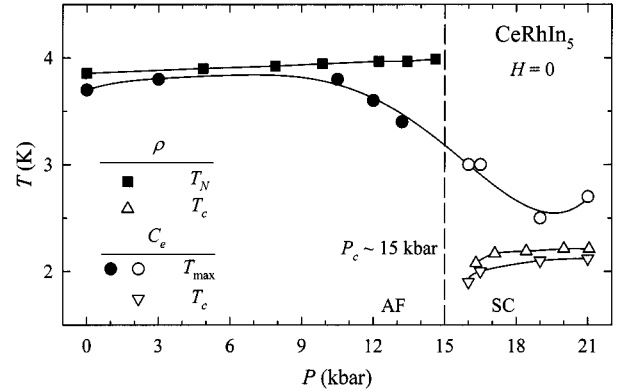


**Fig. 2.** Phase diagram for  $\text{CeRhIn}_5$  constructed from  $C$  data and  $\rho$  data from Ref. 4 (see text).

in amplitude. A second anomaly, associated with the transition to the SC state, first appears as a small irregularity at 16 kbar (in data that are too close to those at 16.5 kbar to be included in the figures). It grows to a “shoulder” on the magnetic anomaly at 16.5 kbar and reaches its maximum amplitude at 19 kbar. The data permit plausible extrapolations to  $T = 0$ , and the entropy ( $S_e$ ) calculated at 12 K has the same value for all  $P$  to within  $\pm 2\%$ .

Characteristic temperatures derived from  $C_e$  and  $\rho$  are compared in Fig. 2. The temperature of the maximum ( $T_{\text{max}}$ ) of the magnetic anomaly in  $C_e/T$  tracks the  $T_N$  deduced from  $\rho$  (including the small increase at low  $P$ ) for  $P \leq 10$  kbar, but then shifts to lower  $T$ . Values of  $T_c$ , taken as the midpoints of entropy-conserving constructions on  $C_e/T$  (see, e.g., Fig. 3), are in good agreement with the values determined from  $\rho$ , which correspond to the onset of superconductivity.

For  $P = 21$  kbar and  $H = 0, 50,$  and  $70$  kOe, the specific heat is shown in Fig. 3. The values of  $T_c(H)$  obtained from the data do not extend to sufficiently high values of  $H$  to establish unambiguously the form of  $H_{c2}(T)$  over a wide interval in  $T$ , but with the assumption of a parabolic  $T$  dependence they extrapolate to  $H_{c2}(0) = 159$  kOe. For  $T < T_c(H)$ ,  $C_e(H) = \gamma(H)T + B_2(H)T^2$ , and extrapolations to 0 K give the same  $S_e$ ,  $0.99$   $\text{mJ K}^{-1} \text{mol}^{-1}$ , at  $T_c(0)$ , 2.12 K, to within  $\pm 1\%$ . This dependence of  $C_e$  on  $T$  and  $H$  is characteristic of a certain group of heavy-fermion superconductors that includes, e.g.,  $\text{URu}_2\text{Si}_2$  [5] and  $\text{UPt}_3$  [6]. The  $B_2(0)T^2$  term is associated with line nodes in the energy gap and an “unconventional” order parameter [7]. Although line nodes can arise from extended s-wave pairing, they are commonly attributed to a d-wave order parameter in

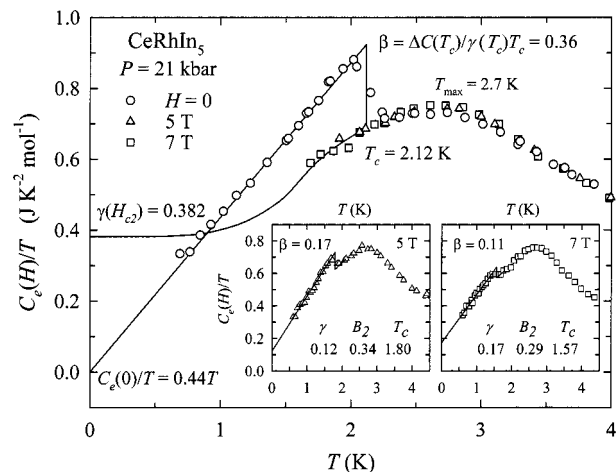


**Fig. 3.**  $C_e(H)$  at 21 kbar. Normal-, mixed-, and superconducting-state data for  $C_e(H)$ , with an extrapolation of the normal-state data to 0 K that is consistent with the SC-state entropy at  $T_c$  and the normal-state  $\gamma$ ,  $\gamma(H_{c2})$  or  $\gamma'(0)$ . The insets show  $C_e(H)$  for 50 and 70 kOe.

HF compounds [7]. The corresponding power-law  $T$  dependence for nuclear-spin relaxation times [7] has been seen [8,9] in NQR measurements. For this pressure, and to within the experimental uncertainty,  $\gamma(0) = 0$  and  $C_e$  in the SC state ( $C_{es}$ ) is  $C_{es} = B_2(0)T^2$ . The value of  $\gamma(0)$  shows that the Fermi surface (except for the line nodes) is fully gapped. For  $T \leq T_c(H)$ ,  $C_e(H)$  and  $S_e(H)$  conform to expectations for SC material, and any additional contributions to  $C_e$  must be negligible. By that criterion, the superconductivity at 21 kbar is complete as well as bulk.

$C_e$  in the normal state ( $C_{en}$ ) is defined to within narrow limits at 21 kbar (see Fig. 3): For  $T > T_c(H)$ ,  $C_{en}$  is independent of  $H$  and determined by the 70-kOe data to 1.7 K.  $\gamma(H)$  is approximately proportional to  $H$ , and extrapolation to  $H_{c2}(0)$  gives  $\gamma = 382 \text{ mJ K}^{-2} \text{ mol}^{-1}$  for the normal-state value, the 0-K intercept of  $C_{en}/T$  in Fig. 3. (For internal consistency the values of  $\gamma$  and some other parameters are given to more significant figures than warranted by the data.) The interpolation between 1.7 and 0 K must give the same  $S_e(T_c)$  as that given by the data for  $H = 0, 50,$  and  $70$  kOe. The curve in Fig. 3 is a smooth, plausible interpolation that satisfies this condition on the area under the curve. It is almost unique among such possibilities in the sense that any curve that is free of irregular peaks and dips and satisfies this constraint would have to be very similar. Its shape is similar to that of the Kondo singlet-ground-state ordering in some other HF compounds, e.g., URu<sub>2</sub>Si<sub>2</sub> [5] and CeAl<sub>3</sub> [10], and conspicuously different from that

characteristic of AF ordering. Its  $H$  independence also suggests that the “magnetic” anomaly in  $C_e$  is not associated with AF ordering at this pressure.

The discontinuity in  $C_e$  at  $T_c$  is relatively small:  $\beta \equiv \Delta C_e(T_c)/C_{en}(T_c) = [C_{es}(T_c) - C_{en}(T_c)]/C_{en}(T_c)$  is 1.43 for a BCS superconductor and  $\sim 1$  to 1.5 for a number of HF superconductors, but only 0.36 for CeRhIn<sub>5</sub>. However, the small value is a direct consequence of the  $T$  dependence of  $C_{en}$ , the  $T$  dependence of  $C_{es}$ , and the thermodynamic requirement that the entropies of the SC and normal states be equal at  $T_c$ ,  $S_{es}(T_c) = S_{en}(T_c) = S_e(T_c)$ : It requires no independent microscopic interpretation. If  $C_{es} = B_2(0)T^2$  and  $C_{en} = \gamma T$  with  $\gamma$  constant, equality of entropies at  $T_c$  requires that  $\beta = 1$ . For CeRhIn<sub>5</sub>, as for many other HF superconductors,  $C_{en}$  does not correspond to a constant density of quasiparticle states, and must be represented by a  $T$ -dependent  $\gamma'$ , defined by  $C_{en}(T) \equiv \gamma'(T)T$ . In that case,  $\beta = B_2(0)T_c/\gamma'(T_c) - 1$ , which is 0.36 for CeRhIn<sub>5</sub>, as observed. The value of  $\gamma'(0)$  was determined independently, and the interpolation to the value of  $C_{en}/T$  to 1.7 K in Fig. 3 was drawn to satisfy the requirement that  $S_{en}(T_c) = S_{es}(T_c)$ . However, the thermodynamic argument can be turned around to show that the small value of  $\beta$  supports the derived value of  $\gamma'(0)$  and the interpolation: The area under the curve for  $C_{en}/T$  has to be that shown in Fig. 3. CeRhIn<sub>5</sub> is evidently a somewhat extreme case in which  $\gamma'$  is still strongly  $T$  dependent at  $T_c$ , but it is not qualitatively different from, e.g., URu<sub>2</sub>Si<sub>2</sub> for which the deviation of  $\gamma'(T)$  from  $\gamma'(T_c)$  is less precipitous and only 20% at 0 K, and  $\beta \sim 0.9$  [7].

Although the magnetic anomaly in  $C_e$  evolves with increasing  $P$  without a discernable discontinuity in its general shape, the  $T$  dependence of  $C_e$  at low  $T$  is discontinuous at  $P_c$ , as is apparent in Fig. 1a where  $C_e/T$  shows positive curvature for  $P < P_c$ , but zero curvature for  $P > P_c$  as  $T \rightarrow 0$ . For all  $P$ , the lowest-order term in  $C_e$  is  $\gamma(H)T$ . For  $P < P_c$ , the second term is  $B_{AFSW}(H)T^3$  (Fig. 1c), which corresponds to the spin-wave contribution expected for an antiferromagnet; for  $P > P_c$ , it is  $B_2(H)T^2$  (Fig. 1b), which is characteristic of certain heavy-fermion superconductors. With increasing  $P$ ,  $B_{AFSW}(0)$  increases monotonically through the AF region, corresponding to a linear-in- $P$  decrease in the spin-wave stiffness, which is proportional to the product of the moment and the exchange interaction. The  $P$  dependence of  $\gamma(0)$  is displayed in Fig. 4a: The experimental AF values are interpolated to the 21-kbar normal-state value, which was derived from the mixed-state data;

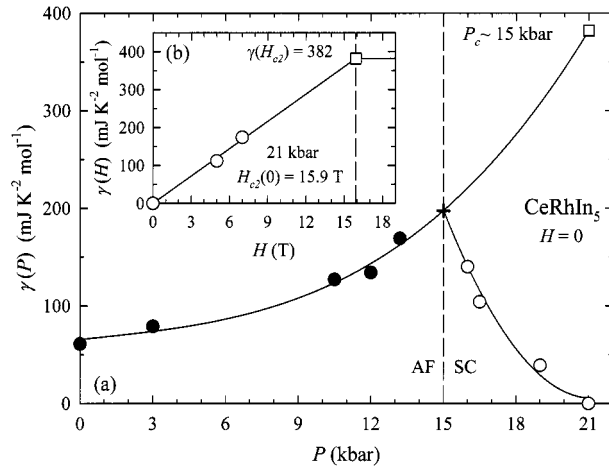


**Fig. 4.** (a) Zero-field values of  $\gamma$  vs.  $P$ . (b)  $\gamma(H)$  vs.  $H$  for  $P = 21$  kbar. In (a) and (b) the open square is the 21-kbar, normal-state value of  $\gamma$  obtained by the extrapolation of the 0-, 50-, and 70-kOe values to  $H_{c2}(0) = 159$  kOe, represented in (b).

the experimental SC values are extrapolated to the AF curve at 15 kbar, the approximate value of  $P_c$  deduced from resistivity measurements [4]. The resulting curves represent a normal-state  $\gamma$ , which measures the density of low-energy quasiparticle excitations, that increases monotonically from ambient pressure to 21 kbar. In zero field and  $P \geq P_c$ , there is a transition to the SC state, but it leaves a “residual”  $\gamma(0)$  that varies between the full normal-state value at  $P_c$  and 0 at 21 kbar.

On the SC side of the phase boundary at  $P_c$ ,  $\gamma(0)$  is the same in the SC and normal states and  $\Delta C_e(T_c) = 0$ . With increasing  $P$ ,  $\gamma(0) \rightarrow 0$  and  $\Delta C_e(T_c)$  increases, but with essentially no increase in  $T_c$ . The extended gapless regions on the Fermi surface of superconductors with  $d_{x^2-y^2}$  pairing [11] suggest a possible basis for understanding this behavior: Below a critical value of the pairing potential the gap vanishes and there is a finite density of low-energy quasiparticle states,  $\gamma(0) \neq 0$ . With increases in the pairing potential the gap appears and increases in amplitude, and the quasiparticle density of states decreases. For sufficiently high gap amplitudes the quasiparticle density of states approaches zero. The observed relation between  $\Delta C_e(T_c)$  and  $\gamma(0)$  would correspond to an increase in the gap amplitude and pairing potential with increasing  $P$ .

Isotherms,  $S_e(P)$  vs.  $P$ , obtained by integration of  $C_e(T)/T$  to obtain  $S_e(T)$  and interpolation to fixed  $T$ 's are shown in Fig. 5. They are related to the volume thermal expansion ( $\alpha$ ), which is proportional to  $(\partial S_e/\partial P)_T$  in magnitude but opposite in sign. Al-

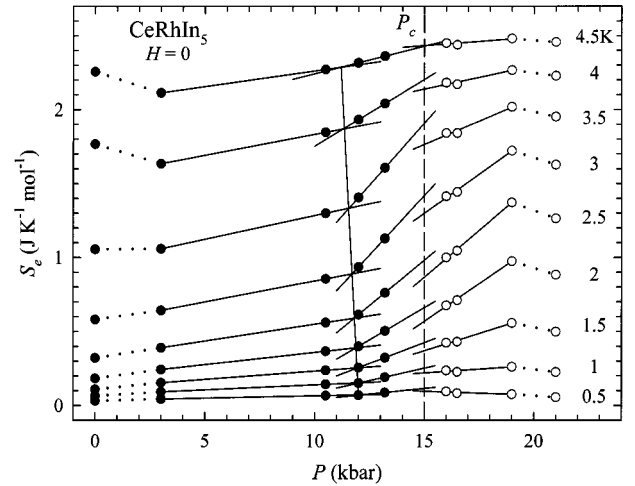


**Fig. 5.** Isotherms of  $S_e(P)$  vs.  $P$  showing features at 12 and 15 kbar which are emphasized by the straight-line approximations (see text).

though the isotherms show that  $\alpha$  is negative in most of the range of  $P$  and  $T$ , they are consistent with the positive values reported [12] at ambient pressure and temperatures above 1 K. The isotherms reveal interesting features near 12 and 15 kbar, which are emphasized in Fig. 5 by three straight-line segments that connect data points in limited intervals of pressure. The straight lines represent discontinuities, in  $(\partial S_e/\partial P)_T$  near 12 kbar and in  $S_e$  at 15 kbar, which correspond to, respectively, second- and first-order thermodynamic transitions. For any one isotherm the features at 12 and 15 kbar represented by the straight lines are comparable in magnitude to the deviations of the points from a smooth curve that might be drawn as an approximate fit to all the points. However, both their systematic variations from one isotherm to the next, which are shown in Fig. 6, and their relation to other properties (see later) attest the reality of structure at least qualitatively similar to that represented by the lines. Furthermore, both discontinuities extrapolate to zero at  $T = 0$ , as required by the third law of thermodynamics, and both tend to small numerical values at temperatures above that of the magnetic ordering, as might be expected if they were associated with the magnetic ordering. The striking similarity of the temperature dependence of  $\Delta(\partial S_e/\partial P)_T$  to that of  $\Delta S_e$  suggests a more direct relation between the two transitions than might be expected for a common origin in the magnetic properties alone, but there is no obvious independent evidence of that.

The feature near 12 kbar, the better defined of the two, is a discontinuity in  $(\partial S_e/\partial P)_T$ , which

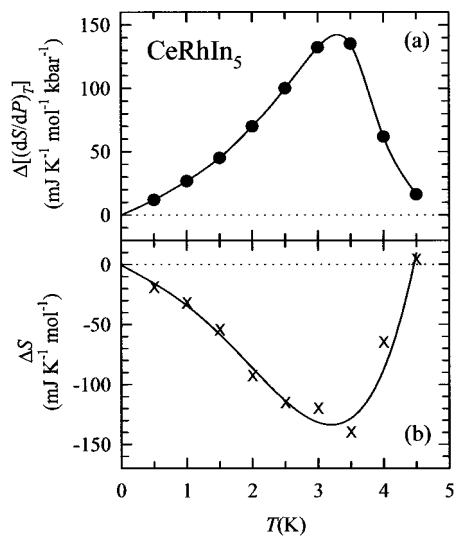


**Fig. 6.** The  $T$  dependence of the features represented by the straight-line approximations to the isotherms in Fig. 5. (a)  $\Delta[(\partial S/\partial P)_T]$  vs  $P$  in the 11–12 kbar region, which corresponds to a second-order transition. (b)  $\Delta S_e$  vs  $P$  at  $P_c = 15$  kbar, which corresponds to a weak first-order transition from the AF to the SC state.

corresponds to a discontinuous increase in the magnitude of  $\alpha$ , which is negative, and a second-order transition. The phase boundary, represented by the nearly vertical solid line in Fig. 5 is defined by the intersections of the straight-line segments of the isotherms, which occur at 12.0 and 11.2 kbar at 0.5 and 4.5 K, respectively. This is a region of the phase diagram in which features in the resistivity and susceptibility have been observed [4], and also where  $T_{\text{max}}$  starts to deviate from its low- $P$  value (see Fig. 2). With the slope of the phase boundary and the Ehrenfest relation, the maximum value of  $\Delta(\partial S_e/\partial P)_T$  gives a maximum discontinuity in  $C$  of  $\sim 50 \text{ mJ K}^{-1} \text{mol}^{-1}$ . The experimental data do not permit a meaningful quantitative comparison, but they are not inconsistent with that value.

The feature at 15 kbar is less well defined, but the points above and below 15 kbar cannot be connected by smooth curves without a change in sign of the curvature. The vertical dashed line in Fig. 5 represents a phase boundary at  $P_c = 15$  kbar, as defined by the construction in Fig. 4, and taken to be independent of  $T$ . The straight-line representations of the isotherms then correspond to a finite  $\Delta S_e$  at  $P_c$ , and a first-order transition from a low- $P$  phase, which must have the larger volume, to a high- $P$  phase that has a lower  $S_e$ . The values of  $-\Delta S_e$  reach a maximum,  $\sim 0.13 \text{ J K}^{-1} \text{mol}^{-1} = 0.022 \text{ RIn}_2$ , near 3 K, and extrapolate to 0 near 4.5 K. At 1 K and below, they correspond, to within a factor of 2, to the extrapolations to  $P_c$  of the low- $T$  terms in  $C_e$ . The vertical phase boundary drawn in Fig. 2 would imply zero change in volume at  $P_c$ ; a slope of  $2 \text{ K kbar}^{-1}$  would correspond to a maximum fractional change in volume of  $\sim 3 \times 10^{-5}$ . This interpretation of the isotherms corresponds to a transition from the AF state to the SC state that includes a small first-order component, which terminates at a critical point in the vicinity of the magnetic ordering temperature. It is supported by its consistency with other properties of the system as well as by the systematic variation with  $T$  of the values of  $\Delta S_e$  obtained by the straight-line constructions in Fig. 5. The plausibility of this interpretation of the isotherms notwithstanding, it must be recognized that the points on the isotherms are not sufficiently closely spaced in  $P$  to define precisely the interval in which the  $\Delta S_e$  occurs. The data do not distinguish between a “sharp” transition that takes place in a few 10ths of a kilobar, a width that might be attributed to sample and pressure inhomogeneities, and a broader feature in  $S_e$  that is not a thermodynamic phase transition. In the latter case the values of  $\Delta S_e$  would be measures of the discrepancies between the values of  $S_e$  at  $P_c$  obtained by extrapolations from higher and lower pressures. However, as such, they would still be relevant to understanding the “transition.” Furthermore, they would put an upper limit to the entropy discontinuity accompanying any “real” first-order transition.

ACKNOWLEDGMENTS

We are grateful to A. V. Balatsky and V. Z. Kresin for helpful discussions. The work at LBNL was supported by the Director, Office of Basic Energy Sciences, Materials Sciences Division of the U.S. DOE under Contract No. DE-AC03-76SF00098. The work at LANL was performed under the auspices of the U.S. DOE. Z. Fisk acknowledges support through NSF Grant Nos. DMR-9870034 and DMR-9971348.

## REFERENCES

1. S. Doniach, in *Valence Instabilities and Related Narrow Band Phenomena*, R. D. Parks, ed. (Plenum, New York, 1977), p. 169.
2. N. D. Mathur, F. M. Grosche, S. R. Julian, I. R. Walker, D. M. Freye, R. K. W. Haselwimmer, and G. G. Lonzarich, *Nature (London)* **394**, 39 (1998).
3. S. S. Saxena, P. Agarwal, K. Ahilan, F. M. Grosche, R. K. W. Haselwimmer, M. J. Steiner, E. Pugh, I. R. Walker, S. R. Julian, P. Monthoux, G. G. Lonzarich, A. Huxley, I. Sheikin, D. Braithwaite, and J. Flouquet, *Nature (London)* **406**, 587 (2000).

4. H. Hegger, C. Petrovic, E. G. Moshopoulou, M. F. Hundley, J. L. Sarrao, Z. Fisk, and J. D. Thompson, *Phys. Rev. Lett.* **84**, 4986 (2000).
5. R. A. Fisher, S. Kim, Y. Wu, N. E. Phillips, M. W. McElfresh, M. S. Torikachvili, and M. B. Maple, *Physica B* **163**, 419 (1990).
6. R. A. Fisher, S. Kim, B. F. Woodfield, N. E. Phillips, L. Taillefer, K. Hasselbach, J. Flouquet, A. L. Giorgi, and J. L. Smith, *Phys. Rev. Lett.* **62**, 1411 (1989).
7. R. H. Heffner and M. R. Norman, *Comments Cond. Mat. Phys.* **17**, 325 (1996).
8. T. Mito, S. Kawasaki, G.-Q. Zheng, Y. Kawasaki, K. Ishida, Y. Kitaoka, D. Aoki, Y. Haga, and Y. Onuki, *Phys. Rev. B* **63**, 220507(R) (2001).
9. Y. Kohori, Y. Yamato, Y. Iwamoto, and T. Kohara, *Euro. Phys. J.* **18**, 601 (2000).
10. G. E. Brodale, R. A. Fisher, N. E. Phillips, J. Flouquet, and C. Marcenat, *J. Magn. Magn. Mater.* **54-57**, 419 (1986).
11. S. Haas, A. V. Balatsky, M. Sigrist, and T. M. Rice, *Phys. Rev. B* **56**, 5108 (1997).
12. T. Takeuchi, T. Inoue, K. Sugiyama, D. Aoki, Y. Tokiwa, Y. Haga, K. Kindo, and Y. Onuki, *J. Phys. Soc. Jpn.* **70**, 877 (2001).